The 2025 World Congress on
Advances in Structural Engineering and Mechanics (ASEM25)
BEXCO, Busan, Korea, August 11-14, 2025

Optimizing Water-Proof Grouting in Tunnels Affected by Excavation Damage Zones

*Lymeng Ny[1], Joon-Shik Moon[2] and Hyoung-Seok Oh[3]

[1), 2), 3)] *Department of Civil Engineering, Kyungpook National University, Daegu 41566, Republic of Korea*
[2)] *j.moon@knu.ac.kr*

ABSTRACT

Utilizing efficient grouting through a numerical approach reduces groundwater inflow into tunnels with Excavation Damage Zones (EDZs). EDZs, resulting from stress redistribution during tunnel excavation, significantly increase the permeability of the surrounding rock and present a substantial risk to tunnel stability. This study proposes a new analytical equation that models water inflow into circular tunnels by considering the combined effects of intact rock, EDZ, and grouted zones as a series of hydraulic resistances. To verify the proposed model, numerical simulations using PLAXIS 2D were conducted under varying rock conditions, grouting thicknesses, and permeability reduction factors. The results show that effective grouting can decrease inflow water volumes by over 90% with low-permeability grout. Moreover, this research suggests that lower-grade rock types require greater quantities of grout for effective sealing. Analytical models offer reasonable preliminary estimates; however, numerical simulations are more reliable and relevant to the actual site conditions. This establishes a practical and optimized framework for grouting design throughout the entire process, enhancing tunnel safety in water-burdened construction scenarios.

1. INTRODUCTION

Water ingress into deep tunnels is one of the most pressing issues in tunnel excavation, particularly while driving through weathered and fractured rock masses. The mechanical excavation process generates a redistribution zone of stress on the tunnel periphery, commonly referred to as the Excavation Damage Zone (EDZ). It is characterized by microcracking, reduced cohesion, loss of confining pressure, and an extreme rise in permeability, all of which tend to enhance groundwater flow into the tunnel lining (Martino and Chandler 2004; Tsang, Bernier, and Davies 2005). The development

---

[1)] Master Student
[2)] Professor (Corresponding Author)
[3)] Doctoral Candidate

of an EDZ compromises the rock mass's mechanical integrity. It poses severe hydrogeological threats in the form of uncontrolled groundwater inflow, reduced tunnel stability, and increased long-term maintenance costs.

The interaction between groundwater and the EDZ is particularly significant. During excavation, the stress relief at the tunnel boundary promotes the extension of cracks and the opening of existing fractures. These conduits are preferential pathways for groundwater seepage, leading to severe engineering problems such as tunnel face instability, flooding, and extended construction durations (Perras and Diederichs 2016). However, studies such as Fernandez and Moon (2010) have shown that the excavation process may also lead to localized closure of joints, reducing permeability in certain cases. This dual behavior highlights the complex and site-specific nature of hydro-mechanical interactions in EDZs. Groundwater flow into tunnels also affects structural support systems. Prolonged exposure to water may lead to corrosion of steel reinforcement and the degradation of shotcrete or concrete lining, thereby weakening their load-bearing capacity (Butscher, Huggenberger, and Zechner 2011). Even under conditions of high-pressure groundwater, water penetration may cause uplift, hydraulic fracturing, or erosion at the tunnel invert and face. Countermeasures should be implemented to mitigate these risks and ensure safety and stability.

One of the most widely used and effective countermeasures is grouting: the installation of a cementitious, chemical, or composite grout material in the soil to reduce permeability, plug fractures, and enhance ground strength. Grouting serves a dual role as a hydraulic and structural reinforcing material, resisting water inflow and aiding tunnel lining support throughout and after the excavation process (Axelsson, Gustafson, and Fransson 2009; Bruce 2005). While it is widely applied, the design and use of grouting methods are often empirical or based on trial and error, which can lead to less-than-optimal performance, excessive material consumption, or underperformance in poor ground conditions. Systematic and predictive optimization of grouting remains a significant challenge in research and engineering.

However, a significant gap in the literature is the lack of integrated frameworks that combine EDZ geometry estimation, groundwater inflow prediction, and grouting optimization into a single model. Most studies tend to focus on just one aspect: either inflow prediction, EDZ, or grout performance, without considering their interactions as a whole. Additionally, many numerical models require extensive calibration, while analytical models may oversimplify the effects of excavation-induced permeability changes. Therefore, there is an urgent need for a hybrid analytical-numerical approach that addresses the impacts of coupled excavation, hydraulic flow, and grouting intervention calibrated with actual data and grounded in a robust theoretical framework.

To address these limitations, the current research proposes an integrated method for numerically optimizing grouting to reduce groundwater inflow in tunnels affected by the EDZ. The objective is to estimate the thickness of the EDZ using empirical and analytical techniques, simulate groundwater flow using PLAXIS 2D, and analyze the effects of various grout parameters, such as thickness and permeability, on inflow rates. This study combines well-established inflow equations with modeling and provides a platform to identify optimal grouting strategies that ensure tunnel stability while minimizing material usage and costs.

2. ANALYTICAL SOLUTIONS

The optimization process for selecting the most appropriate grouting parameters systematically incorporates empirical estimation, numerical simulation, and iterative optimization. The process begins with the calculation of EDZ thickness using empirical methods and progresses to numerical simulations to evaluate the optimum permeability and thickness of grouting. **Fig. 1** presents a step-by-step workflow outlining this method.

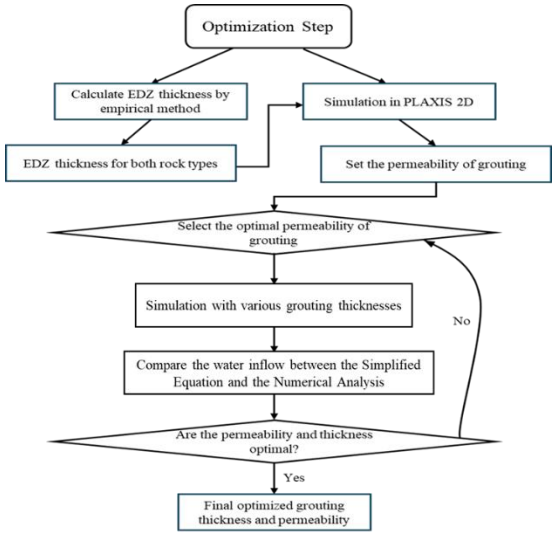

Fig. 1 Optimization process for selecting the best grouting permeability and thickness using empirical methods and numerical simulation

2.1. Analytical EDZ thickness based on the empirical method

The Excavation Damage Zone (EDZ) forms around tunnels due to mechanical disturbance and stress redistribution during excavation. The zone is characterized by increased fracture density, permeability, and reduced strength, all of which affect tunnel stability and groundwater ingress. Proper assessment of the EDZ is crucial in tunneling projects, especially under hydrogeological stress.

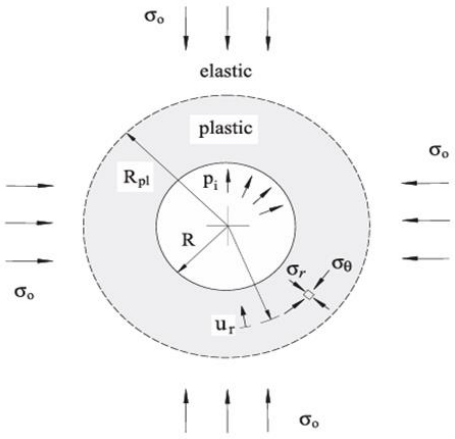

Fig. 2 The circular tunnel is made of elastic plastic and is subject to uniform loading

2.1.1. The Hoek-Brown Failure Criterion

The Hoek-Brown failure criterion is an empirical relationship for estimating the shear strength of rock masses. It originates from intact rock and has been generalized to encompass the effects of rock mass structure, discontinuities, and excavation damage. This makes it particularly suitable for tunnel engineering, especially for determining the Excavation Damage Zone (EDZ). The generalized Hoek-Brown criterion for rock masses, incorporating the Geological Strength Index (GSI) and the disturbance factor (D), is expressed as:

$$\boldsymbol{\sigma_1 = \sigma_3 + \sigma_{ci}\left(m_b \frac{\sigma_3}{\sigma_{ci}} + s\right)^{\alpha}} \tag{1}$$

Where:

$$\boldsymbol{m_b = m_i exp\left(\frac{GSI-100}{28-14D}\right)} \tag{2}$$

$$\boldsymbol{\delta = exp\left(\frac{GSI-100}{9-3D}\right)} \tag{3}$$

$$\boldsymbol{\alpha = 0.5 + \frac{1}{6}\left[exp\left(\frac{-GIS}{15}\right) - exp\left(\frac{-20}{3}\right)\right]} \tag{4}$$

This generalized form enables the criterion to be applied to fractured and weathered rock masses commonly encountered in tunnel projects.

2.1.2. Transformation of Hoek-Brown

Londe (1988) first converted the effective stress form of Eq.(**1**), normalizing each term concerning $m_i\sigma_{ci}$, then rearranged the equation to produce a dimensionless form:

$$\boldsymbol{S_1 = S_3 + \sqrt{S_3}} \tag{5}$$

Where S_1 and S_3 are the principal stresses σ_1 and σ_3, transformed as follows:

$$\boldsymbol{S_1 = \frac{\sigma_1}{m_b^{(1-\alpha)/\alpha}\,\sigma_{ci}} + \frac{s}{m_b^{1/\alpha}}} \tag{6}$$

$$\boldsymbol{S_3 = \frac{\sigma_3}{m_b^{(1-\alpha)/\alpha}\,\sigma_{ci}} + \frac{s}{m_b^{1/\alpha}}} \tag{7}$$

Considering Eq.(6) and (7), the rock mass failure criterion, as expressed in Eq. (**1**), can now be conveniently rewritten as:

$$\boldsymbol{S_1 = S_3 + \mu S_3^{\alpha}} \tag{8}$$

2.1.3. Calculation of Plastic Zone

The Hoek-Brown parameters are applied to convert the stress components associated with the problem illustrated in Fig. 2, as will be described in Section 2.1.2. The stresses below have been transformed using the Peak properties of the Hoek-Brown criterion:

$$\boldsymbol{S_0 = \frac{\sigma_0}{m_b^{(1-\alpha)/\alpha}\sigma_{ci}} + \frac{s}{m_b^{1/\alpha}}} \tag{9}$$

$$\boldsymbol{P_i = \frac{p_i}{m_b^{(1-\alpha)/\alpha}\sigma_{ci}} + \frac{s}{m_b^{1/\alpha}}} \tag{10}$$

$$\boldsymbol{P_i^{cr} = \frac{p_i^{cr}}{m_b^{(1-\alpha)/\alpha}\sigma_{ci}} + \frac{s}{m_b^{1/\alpha}}} \tag{11}$$

The following are transformed stresses using Residual Hoek-Brown properties:

$$\boldsymbol{\tilde{S}_0 = \frac{\sigma_0}{m_b^{(1-\alpha)/\alpha}\sigma_{ci}} + \frac{\tilde{s}}{m_b^{1/\alpha}}} \tag{12}$$

$$\boldsymbol{\tilde{P}_i = \frac{p_i}{m_b^{(1-\alpha)/\alpha}\sigma_{ci}} + \frac{\tilde{s}}{m_b^{1/\alpha}}} \tag{13}$$

$$\boldsymbol{\tilde{P}_i^{cr} = \frac{p_i^{cr}}{m_b^{(1-\alpha)/\alpha}\sigma_{ci}} + \frac{\tilde{s}}{m_b^{1/\alpha}}} \tag{14}$$

In the preceding equations, σ_0 and p_i represent the far-field stress and the internal support pressure acting on the tunnel walls, respectively. The parameter p_i^{cr} denotes the critical internal pressure threshold, below which a plastic zone of radius R_p forms around the tunnel.

From the similarity approach, as proposed by Carranza-Torres and Fairhurst (1999), P_i^{cr} critical internal pressure, transformed by peak properties, can be obtained through the solution of the following transcendental equation:

$$\boldsymbol{\mu P_i^{cr^\alpha} + 2P_i^{cr} - 2S_0 = 0} \tag{15}$$

Indeed, an exact closed-form solution of the above equation is possible only for the particular case $\alpha = 0.5$:

$$\boldsymbol{P_i^{cr} = \left[\frac{1-\sqrt{1+16S_0}}{4}\right]^2} \tag{16}$$

By using Eq.(**16**), the transformed value of P_i^{cr} can be obtained; then, the actual internal pressure p_i^{cr} will be derived by inverting Eq.(**11**), as:

$$\boldsymbol{p_i^{cr} = \left[P_i^{cr} - \frac{s}{m_b^{1/\alpha}}\right] m_b^{(1-\alpha)/\alpha}\sigma_{ci}} \tag{17}$$

The equilibrium equation in the radial direction for an axisymmetric problem is:

$$\frac{d\sigma_r}{dr} + \frac{\sigma_r - \sigma_\theta}{r} = 0 \tag{18}$$

The distribution of transformed hoop stress:

$$\tilde{S}_\theta = \tilde{S}_r + \tilde{\mu}\tilde{S}_r^{\tilde{\alpha}} \tag{19}$$

Where $\tilde{\mu} = \tilde{m}_b^{(2\tilde{\alpha}-1)/\tilde{\alpha}}$
Substituting Eq.(19) into Eq.(18):

$$\frac{d\tilde{S}_r}{dr} = \frac{\tilde{\mu}\tilde{S}_r^{\tilde{\alpha}}}{r} \tag{20}$$

The separation of variables can solve Eq.(**20**):

$$\frac{\tilde{S}_r^{(1-\tilde{\alpha})}}{1-\tilde{\alpha}} = \tilde{\mu} ln(r) + C \tag{21}$$

By applying boundary conditions at $r = R_p$ where $S_r = P_i^{cr}$ and at the tunnel wall $r = R$, where $S_r = P_i$, after applying these conditions to Eq.(21), we have:

$$\frac{\tilde{P}_i^{cr^{(1-\tilde{\alpha})}} - \tilde{P}_i^{(1-\tilde{\alpha})}}{1-\tilde{\alpha}} = \tilde{\mu} ln\left(\frac{R_p}{R}\right) \tag{22}$$

$$R_p = Rexp\left[\frac{\tilde{P}_i^{cr^{(1-\tilde{\alpha})}} - \tilde{P}_i^{(1-\tilde{\alpha})}}{(1-\tilde{\alpha})\tilde{\mu}}\right] \tag{23}$$

2.2. Simplified for Estimating Water Inflow with EDZ and Grouting Conditions

Previous research on groundwater inflow through a tunnel has generally addressed either the effect of the Excavation Damage Zone (EDZ) or the grouting effect, but not both simultaneously. Analytical models by Goodman et al. (1964), Karlsrud (2002), and Mohamed El Tani (2003) estimate water inflow using simple conditions but overlook the higher permeability from EDZs. Similarly, grouting models by Chen et al. (2024), Wang et al. (2008), and Ying et al. (2016) deal with water inflow reduction without taking into account the altered hydraulic conditions caused by excavation damage. Therefore, existing research does not explain the combined effect of EDZ and grouting. This article fills that gap by integrating both factors into a single model to forecast groundwater inflow more accurately and design effective grouting.

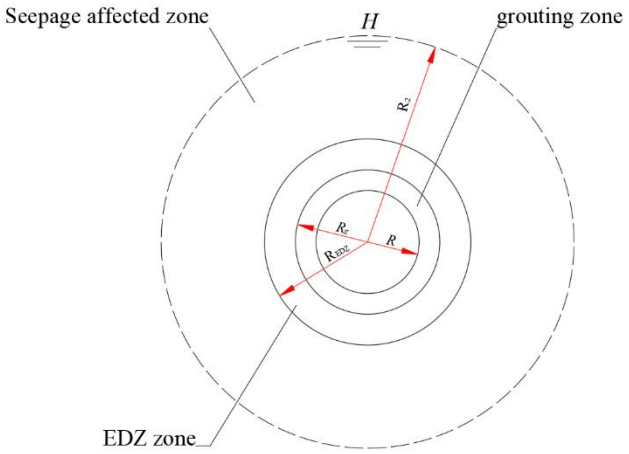

Fig. 3 Calculation Model

The calculation model illustrated in **Fig. 3** is a simplified representation used to analyze groundwater flow through the EDZ and grouted zone. In this model, R denoted the tunnel radius, R_g is represents the radius of the grouting zone, R_{EDZ} is the radius of the EDZ zone, and R_2 corresponds to the effective radius of influence.

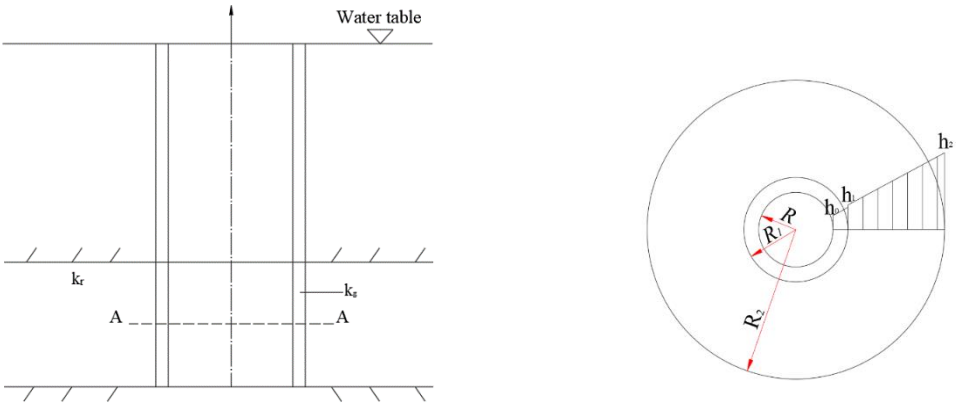

(a) Schematic plan of the Well (b) A-A Section

Fig. 4 Schematic plan of the Well

Fig. 4 illustrates a conceptual model of radial flow towards a tunnel, represented by a well with an inner radius R and an outer radius R_g. The equivalent hydraulic heads at these points and the far-field boundary are h_0, h_1, and h_2, respectively. The hydraulic conductivities of rock and the grout are k_r and k_g, respectively. The surrounding aquifer in the vicinity is considered to be a homogeneous, isotropic, confined aquifer with uniform thickness and infinite horizontal extent. Groundwater flow is horizontal and permanent, governed by Darcy's law under these assumptions.

The governing equation for radial flow in cylindrical coordinates is given by:

$$\frac{d}{dr}\left(r\frac{dh}{dr}\right)=0 \tag{24}$$

According to Darcy's law, discharge through a cylindrical surface in the rock mass is:

$$Q=2\pi r k_r\frac{dh}{dr} \tag{25}$$

Following
Fig. **4** (b), integrating between the boundaries R_2 and R_{g}, with corresponding heads h_2 and h_1:

$$Q_1=\frac{2\pi k_r(h_2-h_1)}{ln\left(\frac{R_2}{R_g}\right)} \tag{26}$$

Similarly, discharge through tunnel grouting (R to R_g) is:

$$Q_2=\frac{2\pi k_g(h_1-h_0)}{ln\left(\frac{R_g}{R}\right)} \tag{27}$$

Assuming continuity of flow ($Q_1=Q_2=Q$), and $h_0=0$; solving for h_1:

$$h_1=\frac{h_2 ln\left(\frac{R_g}{R}\right)}{\frac{k_g}{k_r}ln\left(\frac{R_2}{R_g}\right)+ln\left(\frac{R_g}{R}\right)} \tag{28}$$

Substituting Eq.(28) back into Darcy's equation gives the total discharge:

$$Q=\frac{2\pi k_g h_1}{ln\left(\frac{R_g}{R}\right)}=\frac{2\pi k_r h_2}{\frac{k_r}{k_g}ln\left(\frac{R_g}{R}\right)+ln\left(\frac{R_2}{R_g}\right)} \tag{29}$$

Letting $h_2=H$ (full hydraulic head), so Eq.(29) is:

$$Q=\frac{2\pi k_r H}{\frac{k_r}{k_g}ln\left(\frac{R_g}{R}\right)+ln\left(\frac{R_2}{R_g}\right)} \tag{30}$$

When an EDZ zone exists between the grouting and the surrounding rock, the head losses across the three layers are described as:

$$\frac{2\pi k_r(H-h_{EDZ})}{ln\left(\frac{R_2}{R_{EDZ}}\right)}=\frac{2\pi k_{EDZ}(h_{EDZ}-h_1)}{ln\left(\frac{R_{EDZ}}{R_g}\right)}=\frac{2\pi k_g(h_1-h_0)}{ln\left(\frac{R_g}{R}\right)} \tag{31}$$

This setup can be interpreted as three hydraulic resistances in series. By analogy with electrical circuits, the total head loss is the sum of head losses across each zone, giving the total discharge:

$$Q = \frac{2\pi k_r H}{ln\left(\frac{R_2}{R_{EDZ}}\right) + \frac{k_r}{k_{EDZ}} ln\left(\frac{R_{EDZ}}{R_g}\right) + \frac{k_r}{k_g} ln\left(\frac{R_g}{R}\right)} \quad (32)$$

The Eq.(32) incorporates the effects of variable permeability and the thickness of the EDZ and grouting layer, enabling improved inflow predictions under complex geology conditions. Its structure reflects the combined resistance to flow as a series of logarithmic terms, similar to series resistors, making it a convenient and theoretically sound approach for evaluating and optimizing grouting schemes to reduce water entry in EDZ-affected tunnels.

3. PARAMETRIC FOR STUDY

The parametric study conducted in this research is based on Table 1 and Table 2. The rock type is Tuff, which is why the m_i value is set to 18, established through site inspections and laboratory experimentation. It is assumed that the material behaves as perfectly plastic, and the tunnels are unsupported $(p_i = 0)$. For this study, a theoretical and numerical analysis was designed for a 5 m radius circular TBM tunnel located at 50 m. The EDZ thicknesses used in this study were also calculated based on Eq. (23) and the rock properties in Table 2. A series of grouting permeability reduction ratios (1/10, 1/20, 1/50, and 1/100) is used to analyze the sensitivity of inflow to the efficiency of grout in groundwater. The grouting thickness is also varied from 0.5 m to 2.0 m to compare its contribution to reducing inflow under steady-state seepage conditions

Table 1. Rock Mass's properties used in the parametric study

Rock Grade	Unit weight (kN/m^3)	Cohesion (KPa)	Poisson's Ratio	Friction angle	Elastic modulus (MPa)
I	27.00	3,600	0.20	46.7	22,800
II	26.00	2,700	0.22	42.8	13,500
III	25.00	1,500	0.24	38.6	6,300
IV	23.00	620	0.26	34.7	3,200
V	22.00	150	0.28	32.3	700

Table 2. Hoek-Brown criteria physical and mechanical parameters

Rock Grade	m_i	GSI	Uniaxial Compressive Strength (MPa)	Lateral Pressure Coefficient	Permeability (cm/s)
I	18	82	106.00	0.52	9.4×10^{-7}
II	18	67	81	0.53	3.7×10^{-6}
III	18	54	62	0.55	1.0×10^{-5}
IV	18	35	37	0.57	2.5×10^{-5}
V	18	25	21	0.58	3.9×10^{-5}

4. NUMERICAL METHOD

A numerical model is developed to validate the approximate analytical solution by simulating the groundwater flow process around the tunnel. The numerical analysis is carried out using PLAXIS 2D, an FEM-based software widely used for geotechnical and hydrogeological analysis. PLAXIS 2D is well-suited for simulating complicated interactions between soil and structure, and it can look at both steady-state and changing groundwater flow conditions.

As shown in **Fig. 5**, the modelling comprises a tunnel with a radius of 5 meters at a depth of 50 meters, with the groundwater level set 35 meters above the tunnel crown. The behavior of the rock mass is described using the Mohr-Coulomb failure criterion, while the EDZ is simulated using reduced permeability values obtained through empirical estimation. Within this study, the EDZ thickness is replaced by the thickness of grouting for simulation purposes.

The numerical model utilizes a steady-state groundwater flow regime, with a constant hydraulic head specified at the far-field boundary and a seepage face condition applied at the tunnel wall to represent groundwater inflow. Mechanical boundary conditions feature roller supports along the vertical boundaries to permit horizontal movement while preventing displacement, along with fixed constraints at the bottom boundary to reflect in-situ stress conditions.

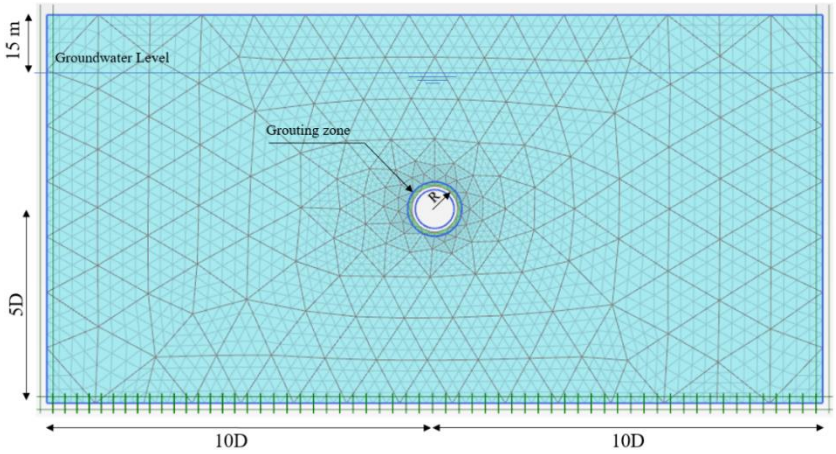

Fig. 5 Modeling for Numerical Analysis

4.1. The Effect of Grouting Permeability

The first condition in this numerical analysis was modeling the thickness of grouting with the same thickness as the EDZ of each rock type. By substituting the tunnel properties condition and the rock mass's properties and parameters listed in Table 1 and Table 2 into Eq.(**23**), the EDZ is equal to the deviator radius. As a result, since rock types I, II, and III are in good rock condition, and from this study, we used the TBM method, the EDZ of these three rocks is zero. On the other hand, Table 3 shows that for rock types IV and V, the EDZ thicknesses are 0.70 m and 2.00 m, respectively.

Table 3. Parameters of computational analyses

Rock Type	R (m)	R_{EDZ} (m)	k_r (cm/s)	k_{EDZ} (cm/s)
IV	5.0	5.7	2.5×10^{-5}	$10 \times k_r$
V	5.0	7.0	3.9×10^{-5}	$10 \times k_r$

The attempts focus on evaluating the different grouting conditions for rock groups IV and V, which are divided into five cases. Along with every case, a schematic is represented using a tunnel cross-section. Case 1 does not have any grouting, and it has the maximum groundwater inflow into the tunnel. Case 2 introduces grouting with reduced groundwater ingress and a permeability ratio of k_g/k_r= 1/10. Then, in Case 3, the ratio is changed to a permeability k_g/k_r = 1/20. However, in Case 4, it is increased to a k_g/k_r= 1/50. Finally, Case 5 employs the most effective permeability decrease with k_g/k_r= 1/100. In these, k_g represents the permeability of the grouted zone, and k_r is the permeability of the surrounding rock mass. These scenarios demonstrate the effectiveness of every method in decreasing the groundwater inflow and improving the tunnel stability in differing geological settings.

4.2. The Effect of the Thickness of Grouting

In this section, numerical analysis was utilized to evaluate the effect of grouting thickness on reducing groundwater inflow in damaged tunnels within EDZs. The case was defined with a specified grouting permeability reduction factor. Grouting thickness was incrementally varied across five cases: (a) 0.5 m, (b) 0.7 m, (c) 1.0 m, (d) 1.5 m, and (e) 2.0 m. The surrounding rock, the grouted zone, and the EDZ were all included in a concentric design, and the analysis considered steady-state groundwater conditions. A constant hydraulic head was applied at the model boundaries, and a seepage face boundary condition was implemented at the tunnel lining to simulate realistic groundwater inflow.

5. RESULTS AND DISCUSSION

The numerical simulation examined the impact of grouting on reducing groundwater inflow in tunnels that experience excavation damage zones (EDZs). The water inflow pattern in tunnels constructed in rock types IV and V varied with different values of the grouted zone's permeability reduction factor and various grouting thicknesses for each rock type. The results demonstrate how different levels of grouting effectiveness impact the tunnel's hydraulic response, confirming that reducing permeability significantly decreases groundwater inflow and enhances tunnel stability.

5.1. Results of grouting permeability

Fig. 6 is illustrated in the graph, showing the effectiveness of grouting in controlling groundwater ingress into the tunnel. Fig. 6 includes groundwater inflow before and after grouting under two grades of rock, V and IV, for different permeability ratios of grouting k_g/k_r. In the initial ungrouted condition, inflow reached 5.608 m³/day/m for rock grade V and rock grade IV 3.616 m³/day/m. With a decrease in grouting permeability (i.e., as

k_g/k_r from 1/10 to 1/100), groundwater inflow decreases significantly in both grades of rock. As shown in Fig. 6 (a), for grade IV rock, as the permeability of grouting decreases, the percentage of water cut off by grouting increases significantly. After applying grout with a permeability ratio 1/10, the inflow decreased by over 66%. Further reductions to 1/20, 1/50, and 1/100 led to inflow reductions of 75%, 86%, and 92%, respectively. This indicates that decreasing the permeability of grouting, which represents a less permeable grouted zone, allows for greater water control Similarly, the effective water inflow into the tunnel, represented by Q_g reduces from 1.239 m³/day/m at k_g/k_r =1/10 to 0.298 m³/day/m at k_g/k_r=1/100. Fig. 6 (b) illustrates the impact of grouting permeability on groundwater inflow reduction for Rock Type V, showing a clear correlation between diminishing grouting permeability and increasing water ingress control. As grouting permeability decreases, represented by lower values of k_g/k_r the percentage of water successfully shut off by grouting rises consistently. At k_g/k_r=1/10, approximately 77% of water inflow is circumvented, while at 1/20, 1/50, and 1/100, the amount increases to 86%, 93%, and 96%, respectively. This trend indicates the effectiveness of lower permeability grouting in limiting water penetration into the tunnel. Concurrently, the observed actual water flow rate into the tunnel Q_g decreases significantly from 1.268 m³/day/m at k_g/k_r=1/10 to as little as 0.203 m³/day/m at k_g/k_r=1/100.

Both rocks follow the same trend, where the lowest permeability grout (k_g/k_r= 1/100) demonstrates the greatest water-blocking efficiency and the least water inflow, while the highest permeability grout (k_g/k_r= 1/10) exhibits poor performance. The corresponding results for both rocks indicate that high-quality, low-permeability grouting materials must be chosen to minimize water inflow into tunnels, regardless of geology.

(a)

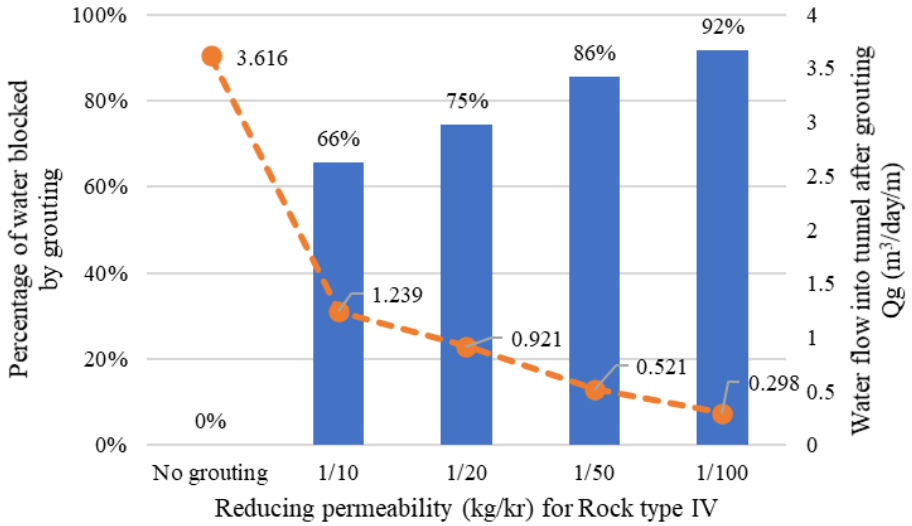

(b)

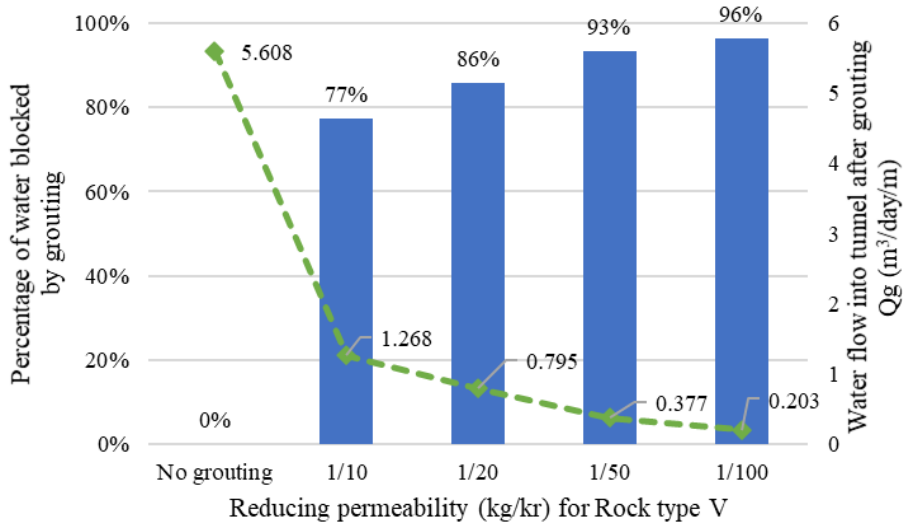

Fig. 6 Water inflow into the tunnel in various grouting permeability (a) Rock type IV and (b) Rock type V

5.2. Results of the effect of the grouting thickness

Based on the discussion in Section 5.1, the grouting permeability k_g/k_r=1/100 has demonstrated the maximum reduction in groundwater inflow and is thus the most suitable case for this section's numerical modeling. Therefore, in the next modeling phase, we will consider this permeability ratio while accounting for the variation in the thickness of grouting to assess its effect on reducing tunnel inflow.

(a)

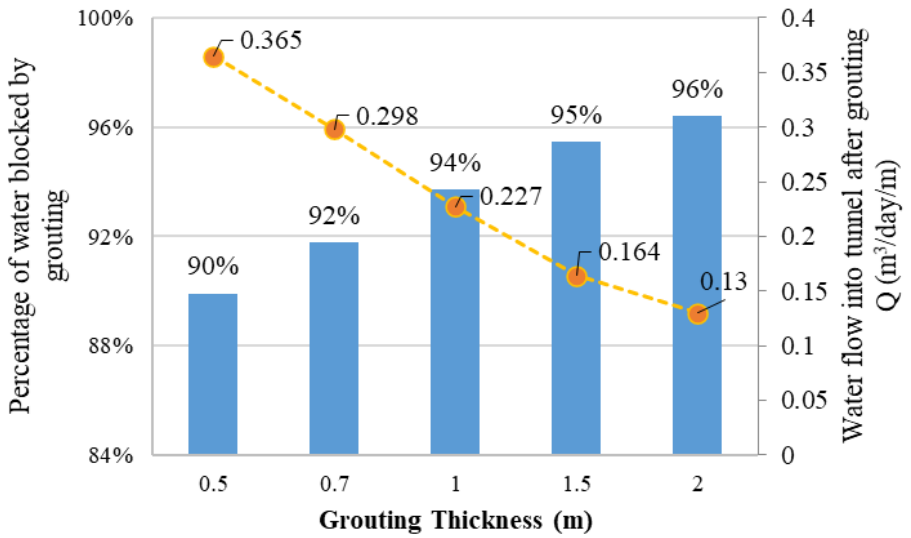

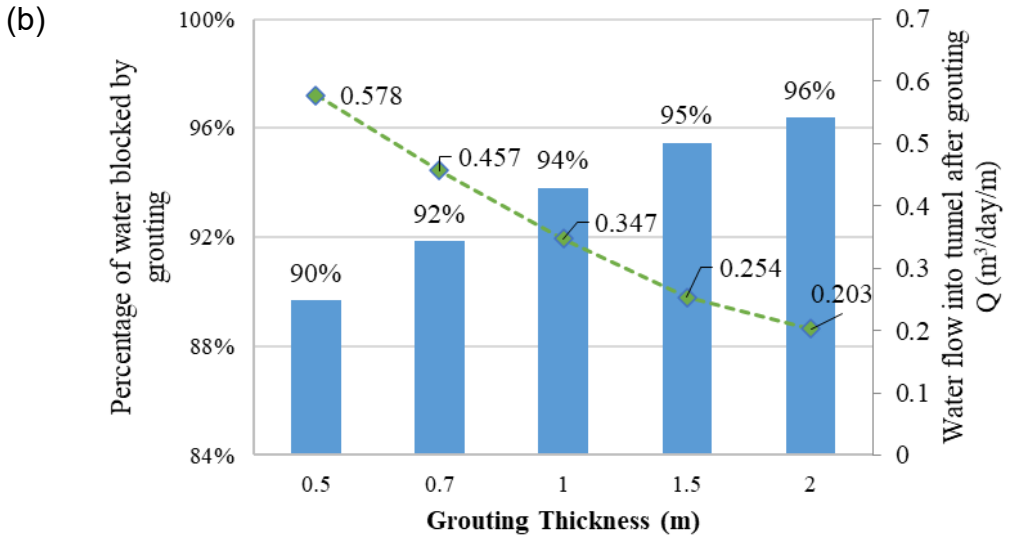

Fig. 7 Water flow into the tunnel in various grouting thicknesses (a) Rock type IV and (b) Rock type V

Fig. 7 illustrates how variations in grouted zone thickness affect the reduction of groundwater inflow when the grout permeability reduction factor is kept constant at k_g/k_r= 1/100, indicating highly effective grouting. Fig. 7 (a), for rock type IV, which has moderately low permeability and better mechanical properties than weaker rocks, even a grouting thickness of 0.7 m achieves considerable inflow reduction. Further increasing the thickness to 1.5 m or 2.0 m enhances this effect, as the inflow rate reduces consistently with the increase in thickness. This indicates that under conditions of moderate geology, relatively thin grout layers combined with high-quality, low-permeability grout can effectively stop water inflow.

As shown in Fig. 7 (b), the same effect is observed for rock type V, which consists of weaker, more fractured rock with higher permeability; however, the reduction in inflow becomes less effective with thinner grouting thicknesses. Increasing the grouting thickness to 2.0 m for rock type V is even more critical, as fewer grout layers (e.g., 0.5 m) cannot provide adequate hydraulic resistance in extremely fractured rock with conducting flow pathways. The conclusion emphasizes that where rock conditions deteriorate, larger grouting thicknesses should be applied to control groundwater to acceptable levels, particularly with high-grade, low-permeability grouting material.

The grout thickness demonstrates a clear relationship with the rate of water ingress, and in cases where the grout was added, the inflow of water decreased significantly. The results show that grouting has reduced water inflow because the grout layers provided a broader barrier.

5.3. Comparison of simplified equation with numerical analysis

As discussed in Section 0 and based on Eq.(**32**), Fig. 8 presents a comparison of water inflow rates into the tunnel after grouting, as calculated with the simplified analytical equation and numerical simulation results under various conditions.

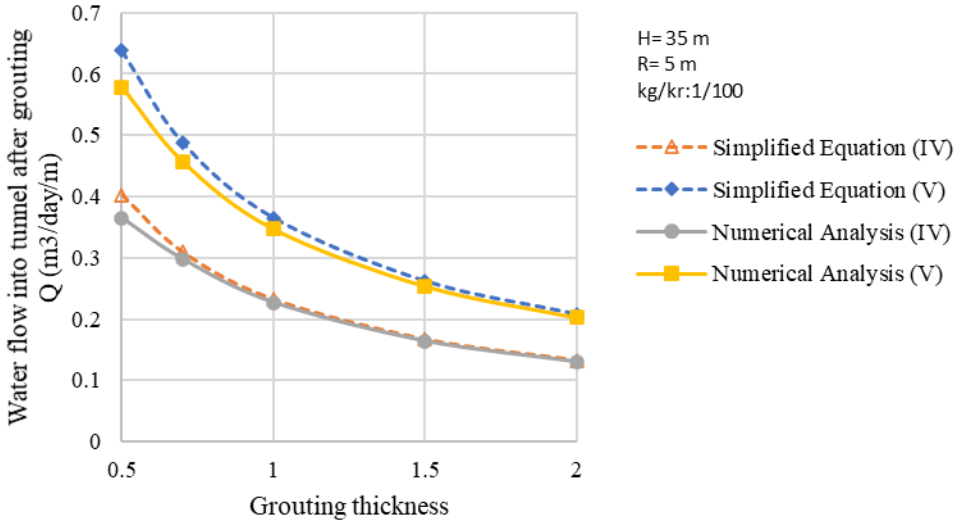

Fig. 8 Comparison of the simplified equation and numerical analyses

The data shows a clear trend for the enhancement of hydraulic resistance Q. As expected, there was less water inflow with greater grouting thickness. According to the numerical results, both scenarios used are in good agreement with the simplified analytical model, particularly for thicker grouting layers (≥ 1.0 m), where the difference becomes negligible. There are some discrepancies with thinner grouting, such as 0.5 m, where the analytical model tends to overpredict inflow compared to the numerical results. This difference can be explained by the assumptions of homogeneity and the lack of local differences in hydraulic gradients near the tunnel boundary made by the analytical model.

5.4. Grouting values and permitted water inflow

The connection between the thickness of the grouting and the permissible amount of groundwater entering tunnels demonstrates a numerical difference for two types of rock impacted by Excavation Damage Zones (EDZs). Simulations showed that under Rock Type IV, which has moderate permeability, a grouting thickness of 0.7 to 1.0 meters was adequate to reduce water inflow by approximately 92-94%, aligning with standard engineering requirements for tunnel waterproofing. In contrast, in highly permeable Rock Type V, thinner grouting (e.g., 0.5 or 0.7 meters) proved insufficient for effective water control. Instead, a thicker application of grouting, ranging from 1.5 to 2.0 meters, was necessary to achieve a 95-96% reduction in groundwater inflow.

These findings align with international tunneling guidelines. For example, permitted groundwater inflow in tunnels is typically limited to 80–95% reduction after grouting (Mao et al. 2016). In sensitive areas like urban environments, allowable limits drop to 2–5 L/min/100 m (H. Stille 2015), while subsea tunnels may allow up to 30 L/min/100 m, depending on geological conditions (K. F. Garshol et al. 2012). Numerical results in this study showed that 0.7–1.0 m grouting in Rock Type IV and 1.5–2.0 m in Rock Type V achieved over 92–96% inflow reduction, aligning well with international standards.

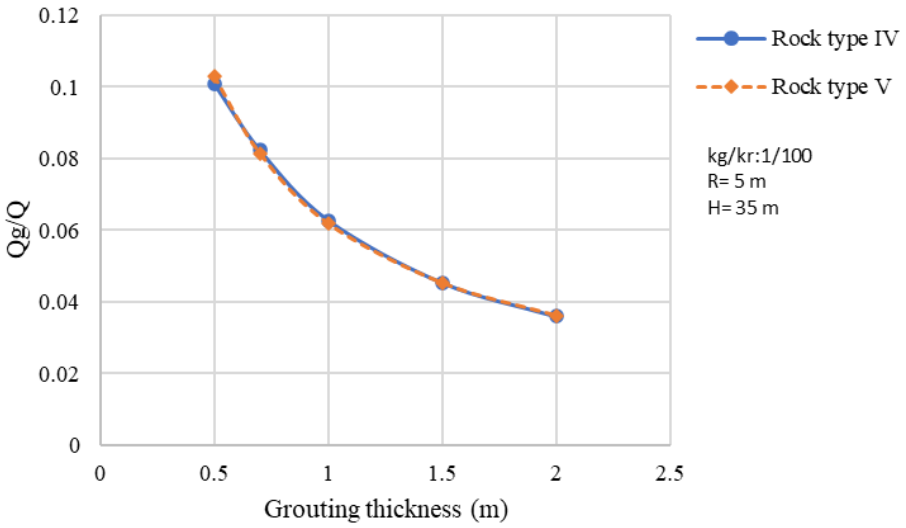

Fig. 9 Comparison of groundwater inflow reduction by grouting thickness in Rock types IV and V

Based on Fig. 9 shows that even though Rock Type IV and Rock Type V have different geological features, especially in how easily water can pass through them and their strength, both types had the same decrease in groundwater inflow when the grouting was improved. This was due to the optimization of grouting thickness and the use of low-permeability grout to meet the requirements of each rock type.

6. CONCLUSIONS

The permeation grouting methods used to control groundwater inflow in tunnels affected by Excavation Damage Zones (EDZs) were subject to numerical optimization as part of this research project. This research incorporated analytical techniques and numerical modeling with PLAXIS 2D, examining the impacts of EDZ thickness, grouting thickness, and permeability reduction on groundwater inflow. The study showed that theoretically estimated results can be reconciled with advanced simulation technology to accurately predict and manage groundwater inflow into tunnels by comparing theoretical approximations with sophisticated numerical modeling.

1) The results underscored that the development of the EDZ has a considerable impact on the permeability of the surrounding rock mass, especially in weaker rock types IV and V. The estimated EDZ thickness for rock type IV was about 0.7 meters and 2.02 meters for rock type V. These zones of high permeability serve as preferential flow conduits for groundwater, which increases the danger of oversaturation, tunnel instability, and delays in construction progress. The studies confirmed that permeation grouting is capable of sealing these degraded zones if the required grout depth and reduction of permeable flow are sufficiently tailored to the geological and hydrological settings.

2) The numerical simulation indicated that Rock Type IV, which is of moderate quality, using 0.7 meters of grouting with a permeability reduction factor of 1/100, decreased groundwater inflow to approximately 0.299 m^3/day/m, compared to 3.616 m^3/day/m without grouting. Applying 2.0 meters of grouting reduced the inflow to around 0.203 m^3/day/m for the lower-quality Rock Type V, in contrast to 5.608 m^3/day/m without it. This demonstrates that both the thickness of grouting and the material's permeability are crucial for minimizing inflow, with reduced permeability being particularly significant in highly fractured rock masses.

3) The correlation between groundwater inflow into the grouted tunnel is accurately predicted using the simplified analytical equation and numerical analysis. The reduction in inflow with increasing grouting thickness is particularly evident and accurately projected by the simplified equation, especially when the zonal permeability contrast is highly dominant and the adjustable inflow region is bounded by rock. Although the model operates under basic flow assumptions such as homogeneity, radial flow symmetry, and low grouting thickness, the reliable predictions from the simplified model support its utility for deeper design evaluations and sensitivity analysis, demonstrating it to be an effective complement to numerical simulations where computations under varying grouting conditions are necessary.

Overall, the study established a comprehensive analytical and numerical platform that provides a pragmatic, science-based solution for optimizing grouting design in tunnels affected by the EDZ. By implementing site-specific EDZ thickness, permeability values, and grouting parameters, the platform enables targeted design adjustments to achieve over 90% inflow reduction under adverse geological conditions. This integrated approach offers insights to tunnel designers, construction engineers, and geotechnical specialists, enhancing groundwater control measures, ensuring the safety of tunnels, and facilitating cost-effective underground construction. Therefore, future studies that combine the most advanced numerical modeling techniques, long-term monitoring data, 3D modeling, and machine learning optimization will further enhance the scientific understanding and daily applicability of grouting solutions to manage groundwater inflow. These studies will contribute to creating safer, more durable, and cost-effective underground infrastructure, particularly in challenging and high-risk geological conditions.

REFERENCES

Axelsson, M., G. Gustafson, and Å. Fransson. 2009. “Stop Mechanism for Cementitious Grouts at Different Water-to-Cement Ratios.” *Tunnelling and Underground Space Technology* 24(4):390–97.

Bruce, Donald A. 2005. “Glossary of Grouting Terminology.” *Journal of Geotechnical and Geoenvironmental Engineering* 131(12):1534–42.

Butscher, Christoph, Peter Huggenberger, and Eric Zechner. 2011. “Impact of Tunneling on Regional Groundwater Flow and Implications for Swelling of Clay–Sulfate Rocks.” *Engineering Geology* 117(3–4):198–206.

Carranza-Torres, C., and C. Fairhurst. 1999. “The Elasto-Plastic Response of Underground Excavations in Rock Masses That Satisfy the Hoek–Brown Failure Criterion.” *International Journal of Rock Mechanics and Mining Sciences* 36(6):777–809.

Chen, Yi-Feng, Jin-Gang He, Wan-Jun Lei, Ran Hu, and Zhibing Yang. 2024. “Optimization Design of Consolidation Grouting Around High-Pressure Tunnel Considering Non-Darcian Flow Effect.” *Rock Mechanics and Rock Engineering* 57(9):7407–24.

Fernandez, G., and J. Moon. 2010. “Excavation-Induced Hydraulic Conductivity Reduction around a Tunnel – Part 1: Guideline for Estimate of Ground Water Inflow Rate.” *Tunnelling and Underground Space Technology* 25(5):560–66.

Goodman, Richard E., Dan G. Moye, A. Van Schalkwyk, and Iraj Javandel. 1964. *Ground Water Inflows During Tunnel Driving*. College of Engineering, University of California.

H. Stille. 2015. *Rock Grouting-Theories and Applications*.

K. F. Garshol, K. W. J. Tam, W. B. S. Mui, K. M. H. Chau, and K. C. K. Lau. 2012. “Grouting Techniques for Deep Subsea Sewage Tunnels in Hong Kong.”

Karlsrud, Kjell. 2002. “Control of Water Leakage When Tunnelling under Urban Areas in the Oslo Region.” *Norwegian Tunnelling Society (NFF)* 27–33.

Mao, Dawei, Ming Lu, Zhiye Zhao, and Melvin Ng. 2016. “Effects of Water Related Factors on Pre-Grouting in Hard Rock Tunnelling.” *Procedia Engineering* 165:300–307.

Martino, J. B., and N. A. Chandler. 2004. “Excavation-Induced Damage Studies at the Underground Research Laboratory.” *International Journal of Rock Mechanics and Mining Sciences* 41(8):1413–26.

Mohamed El Tani. 2003. “Circular Tunnel in a Semi-Infinite Aquifer.” *Tunnelling and Underground Space Technology* 18(1):49–55.

Perras, Matthew A., and Mark S. Diederichs. 2016. “Predicting Excavation Damage Zone Depths in Brittle Rocks.” *Journal of Rock Mechanics and Geotechnical Engineering* 8(1):60–74.

Tsang, Chin-Fu, F. Bernier, and C. Davies. 2005. “Geohydromechanical Processes in the Excavation Damaged Zone in Crystalline Rock, Rock Salt, and Indurated and Plastic Clays—in the Context of Radioactive Waste Disposal.” *International Journal of Rock Mechanics and Mining Sciences* 42(1):109–25.

Wang, Xiuying, Zhongsheng Tan, Mengshu Wang, Mi Zhang, and Huangfu Ming. 2008. “Theoretical and Experimental Study of External Water Pressure on Tunnel Lining in Controlled Drainage under High Water Level.” *Tunnelling and Underground Space Technology* 23(5):552–60.

Ying et al. 2016. “Analytic Solution on Seepage Field of Underwater Tunnel Considering Grouting Circle.” *Journal of Zhejiang University (Engineering Science)* 1018–23.